

Research report

Strength of resting-state functional connectivity associated with performance-adjustment ability



Jinhee Kim*, Eunjoo Kang

Department of Psychology, Kangwon National University, 1 Kangwondaeak-gil, Chuncheon-si, Gangwon-do, 24341 Republic of Korea

ARTICLE INFO

Keywords:

Error adjustment
Dorsal anterior cingulate cortex
Dorsolateral prefrontal cortex
Intrinsic functional connectivity
Individual difference

ABSTRACT

Erroneous behavior is usually, although not always, inhibited following a negative outcome (e.g., a penalty), although this adjusting behavior is highly varied. Here we aimed to identify brain regions associated with successful behavioral adjustment to negative feedback, and the intrinsic functional connectivity associated with individual variability in such adjustments, using combined task-based and resting-state functional magnetic resonance imaging (MRI). Functional MRI data were obtained from 28 young adults performing a visuomotor associative learning task, wherein participants learned by trial and error to make one of four key responses to each of 24 English letters. All preceding error response trials were sorted post hoc, based on whether the error response was repeated (Error-Repeated) or not (Error-Changed) for the subsequent trial with the same stimulus, and the rate of error adjustment for each individual was computed as the number of Error-Changed trials divided by all error trials. We identified two brain regions, the right dorsal anterior cingulate cortex (dACC) and dorsolateral prefrontal cortex (DLPFC), whose brain response was significantly greater for Error-Changed than Error-Repeated trials. Stronger anti-correlation between the right dACC seed and right amygdala and between the DLPFC seed and the paracentral gyrus and inferior temporal region extending to the hippocampus was associated with better adjustment ability. These results suggest that the stronger anticorrelated relationship between the error monitoring region and emotional processing and that between the executive control region with those involved in memory or default mode network reflect individual variability in error adjustment.

1. Introduction

Erroneous behavior is usually, but not always, corrected after a negative outcome. Adjustment of subsequent behavior based on the outcomes of actions is important for adaptive goal-directed behavior, which may be critical for survival. Negative feedback processing for successful behavioral adaptation involves several cognitive processes, including monitoring outcomes [1,2], devoting attentional resources [3], inhibiting erroneous stimulus-response associations [4], and regulating emotional responses evoked by negative outcomes [5]. However, the ability to learn from error varies widely. For instance, individuals with several psychiatric conditions, e.g., depression, addiction, or attention deficit hyperactivity disorder, often experience difficulty in this respect, which can result in significant complications in everyday function [6]. An understanding of the neural mechanisms contributing to this variability is critical for the treatment of such deficits in error processing.

Extensive neurophysiological and neuroimaging studies have shown that the dorsal anterior cingulate cortex (dACC) near the medial

prefrontal cortex (mPFC), pre-supplementary motor cortex, and components of the limbic system, such as the amygdala and insula, are involved during negative feedback processing. In particular, it is well-established through animal and human studies that the dACC/mPFC regions are involved in error processing [1,7–9]. Greater error-related activation in the dACC/mPFC is more likely followed by successful error adjustment, suggesting that those brain regions are associated with performance subsequent to error [10–12]. In addition, the lateral prefrontal cortex, particularly the dorsolateral prefrontal cortex (DLPFC), has been implicated in processing negative performance feedback, and is thought to be involved in the monitoring of executive function, namely working memory. For example, higher DLPFC activity has been reported for negative feedback that was informative for correcting behavior [13]. The aversion network, including the amygdala and the insula, are also related to the emotional aspects of negative feedback processing [14]. Previous studies of dACC activity in relation to individual differences in error adjustment during learning have produced conflicting results, with some reporting relationships between dACC activity and individual variability in learning [15]. For instance,

Abbreviations: CR, correct response; FC, functional connectivity; DLPFC, dorsolateral prefrontal cortex; dACC, dorsal anterior cingulate cortex; mPFC, medial prefrontal cortex

* Corresponding author.

E-mail address: jinheekim@kangwon.ac.kr (J. Kim).

group differences in the feedback-related negativity amplitude of the dACC are observed when comparing two groups assigned based upon reinforcement-learning performance (i.e., learners vs. non-learners) [16,17].

Recently, evidence has emerged to suggest that human cognitive function results from the dynamic interactions of distributed brain regions acting together as networks [18]. Resting-state fMRI is a powerful method for characterizing such networks. With it, functionally connected brain areas have been identified where information flow across distributed cortical systems can be detected [19]. Spontaneous, slow (< 0.1 Hz) frequency fluctuations in BOLD signals are known to be correlated among functionally connected brain regions across time [20,21]. Specifically, one useful strategy is to use the resting activity of one brain region of interest (ROI) to identify other brain regions that are functionally connected (i.e., a seed-based approach). Furthermore, relationships between resting-state functional connectivity (FC) and behavior measurement have been demonstrated to be a powerful tool for investigating individual differences in cognitive function, including perception [22], working memory [23], and language skill [24]. Increased functional integration within networks with similar functions have been reported to be related to the efficiency of cognitive function. In addition, many studies have also shown that enhanced ability in a variety of cognitive functions is also associated with strong negative (i.e. anti-correlated) FC between “task-positive” cognitive networks and “task-negative”, also known as the default mode networks [25–27], usually interpreted as functional segregation for serving competitive or different roles. These findings suggest that both integrated and segregated brain networks may contribute to individual variability in error processing. However, little is known about the functional connectivity that is related to individual variability in error adjustment in a task-independent “at rest” state.

To address these issues, we used combined task-based fMRI and seed-based resting-state FC to identify relevant cognitive processing and neural substrates that are related to individual differences in error adjustment. We utilized event-related fMRI during a learning paradigm, in which participants had to learn stimulus–response associations that were based on outcome information provided by external feedback. To measure individual differences in the efficiency of error processing, we examined the success and failure of negative feedback processing throughout the learning session. We reasoned that its success could be determined only by observing response choices in subsequent trials. Specifically, negative feedback processing of a given trial was considered successful if the response choice for a learning stimulus was switched to an alternative response when the same stimulus was next presented in a subsequent trial, regardless of whether or not the switched response was the target response. Likewise, negative feedback processing of a given trial was considered a failure if the same incorrect response choice was repeated the next time the same stimulus was presented. The efficiency of negative feedback processing was assessed for each participant by calculating the rate of successful behavioral error adjustments. Using event-related fMRI to compare brain activations for negative feedback events with subsequent adjustment (Error-Repeated) to those without (Error-Changed trial), we localized brain regions that were associated with successful error processing during learning. The intrinsic functional connectivity of these brain regions was then identified using the individual differences in error processing efficiency. We then performed a seed-based correlation analysis to find brain regions showing a correlation between individual differences in error adjustment and resting-state FC of two seed brain regions including the dACC and DLPFC that were defined from task-based fMRI results.

Based on previous studies, we hypothesized that FC *between* brain regions that play roles in error processing are at the root of individual variability in error processing. Several factors in FC could be linked to interindividual variability. Integrated FC *within* brain regions that are known to be involved in error and feedback processing can reflect the

efficiency of processing, and result in higher performance in error adjustment. Additionally, it can be assumed that functional segregation between cognitive and emotional processing may ensure that emotion would not interfere with attention. In addition, we predicted that there would be an anti-correlated relationship between the task-positive network and task-negative network (i.e., default mode network), as measured by the strong negative correlation in individuals with better adjustment performance.

2. Material and methods

2.1. Participants

Twenty-eight healthy participants (15 women; mean \pm SD age: 22.5 \pm 2.3 years), recruited from the Kangwon National University community, participated in this study. None reported a history of neurological or psychiatric disorders, and all participants were right-handed. Two were excluded from final analyses due to the inability to follow instructions and inadequate resting-state fMRI acquisition, resulting in 26 participants for the imaging analysis. The study was approved by the institutional review board of Kangwon National University Hospital, and conformed to the tenets of the Declaration of Helsinki. Written informed consent was obtained from each participant before the fMRI scanning session. Participants were given basic payment for participation and a extra monetary bonus, depending on their performance during the fMRI scanning session.

2.2. Behavioral task

During task-related fMRI scanning consisting of four runs, participants performed a feedback-based visuo-motor association learning task in a trial and error fashion: they were told to deduce associations between each letter of the English alphabet and one of four alternative responses (the index and middle finger for each hand). Each trial consisted of the following sequence: All trials started with a fixation “+” for 500 ms; the alphabet stimulus was presented for 2000 ms, followed by a 500-ms fixation inter-stimulus interval; Feedback was shown on-screen for 1500 ms. The inter-trial interval (ITI) was varied between 4 s and 16 s (mean 6000 ms), in order to increase the signal detection in fMRI analysis [28]. The event sequence for each trial is depicted in Fig. 1.

The learning stimuli were composed of 24 letters of the English alphabet. Two alphabet letters, X and O, were excluded from the task to avoid ascribing a pre-existing meaning of correctness (in Korean, X is associated with “incorrect”, and O with “correct”). Each alphabet stimulus was presented eight times during the four runs. For each run, 24 alphabet symbols were presented twice, in a pseudo-random order, with the restriction that the same stimulus never appeared consecutively (average inter-trial delay between the consecutive same stimuli = 253.5 s).

Performance feedback for each trial was provided to indicate whether the participant’s selected response was correct or incorrect. For correct response, monetary positive feedback was always given with the configurations of an upward cone with an incentive of 200 KRW (approximately \$0.20, USD). Since, in the early learning phase the chance of receiving negative feedback was greater than that of positive feedback, in order to avoid large net losses of monetary incentive (although in reality, no subjects were required to pay such a debt) we balanced the 200 KRW reward by varying the size of the penalty (none, 100 KRW, or 500 KRW), using a diamond shape containing ‘X’, a downward cone containing “-100”, or a downward cone containing “-500”, respectively. Each letter used as learning stimulus was associated with a target response in a fixed-rule based fashion, with a fixed size of penalty as negative feedback for incorrect responses.

Participants were instructed to choose a one-button response among the four available in response to a visual learning stimulus presented on

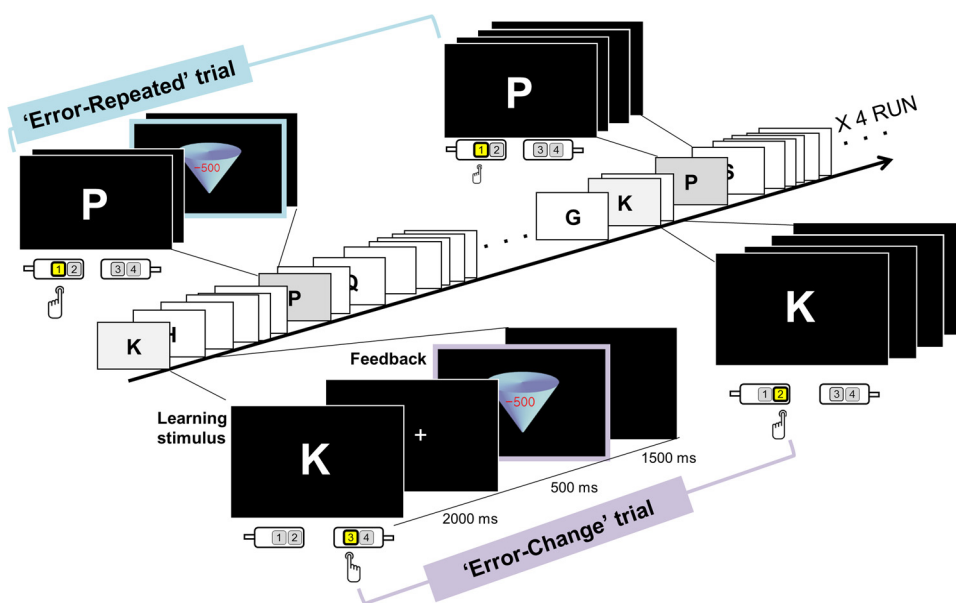


Fig. 1. Experimental paradigm. Participants learned by trial and error to make one of four responses to each of 24 letters of the English alphabet. All error trials were sorted post-hoc, based on whether the error response was repeated ('Error-Repeated') or not ('Error-Change') for the subsequent trial with the same stimulus.

a screen. During a pre-scan training session one week prior to fMRI scanning, participants performed a practice task with Korean letters, to make sure that they were familiar with the behavioral task and the feedback configurations. They were informed that a stimulus-response association would be fixed throughout the learning session, not only for the contingency between stimuli and target response, but also for the amount of monetary loss associated with errors.

Stimulus delivery and response recording were controlled by E-prime (version 2.0, Psychology Software Tools, Inc., Pittsburgh, PA, USA), running on a computer that was interfaced with the MR scanner with an LCD monitor inside the head coil, subtending a visual angle of approximately 15°. To ensure incentive compatibility, participants were informed beforehand that they would receive actual payment based on their performance, and that the total amount of reward/punishment obtained from task performance could be received as an additional bonus. Participants received the financial incentive in cash after finishing the experiments.

2.3. Behavioral analysis

We performed conventional behavioral analyses on the average percentage of correct responses (CR), which was calculated as the percentage of trials with a correct response obtained from the four consecutive runs. To examine whether the S-R association was learned, a one-way repeated measure analysis of variance (ANOVA) was performed on CR rate, with the run (level: 1st, 2nd, 3rd and 4th run) as the within factor using IBM SPSS statistics 20.0 (IBM Corp., Armonk, NY, USA).

"Error adjustment" for a given negative feedback was defined as an instance of switching to a different choice on the next presentation of the same letter, as opposed repeating the same error. An error adjustment rate was calculated from the behavioral data of each individual obtained during the task-based fMRI scans, and the rates for all participants were subjected to a correlation analysis of resting state fMRI data as a covariate. We first selected all trials which were preceded by negative feedback for the same stimulus in a previous trial, and then the choice of behavioral response of the current trial (trial n) was sorted based on the relationship with the previous error. If the current response (trial n) for the same stimulus was switched to an alternative, rather than repeating the response made in the previous trial (trial $n - 1$), it was called an error-changed response. Similarly, if the current

response (trial n) was the same as the previously penalized one (trial $n - 1$), it was called an error-repeated response. Therefore, the response choices of the first presentations of a given stimulus of the first run (there were two presentations of each stimulus in every run) were not included in the behavioral analysis. The error adjustment rate was then calculated for each participant as the ratio of the number of trials with error-changed responses relative to the total number of trials following negative feedback (i.e., the sum of both error-changed and error-repeated responses).

In addition, the length of the delay period (between two consecutive same learning stimuli) was compared between the error-repeated and error-changed trials, in order to evaluate the possibility that it affects the success or failure of subsequent error adjustments.

2.4. MRI acquisition

fMRI data were obtained with a 3-Tesla SIEMENS TRIO scanner in the following order: structural, resting-state fMRI, and task-based fMRI data. T1-weighted anatomical images were obtained using a 3D fast-field echo sequence (repetition time [TR] = 1900 ms, echo time [TE] = 2.52 ms, flip angle = 9°, field of view [FOV] = 256 × 256 mm², matrix size = 256 × 256 × 192, voxel size = 1.0 × 1.0 × 1.0 mm³). The MRI sequence for task-based functional and resting-state imaging was a gradient echo planar imaging (EPI) sequence (TR = 2000 ms, TE = 30 ms, flip angle = 90°, FOV = 240 × 240 mm², 36 slices, descending sequential, 254 volumes, matrix size = 80 × 80, voxel size = 3.0 × 3.0 × 3.0 mm³, 1 mm gap). An fMRI session consisted of one resting-state run and four task-based fMRI runs, each lasting 8 min 28 s. Resting-state was defined as the absence of any specific cognitive task during fMRI scanning, for which subjects were told to relax and close their eyes.

2.5. Task-related fMRI analyses

Preprocessing and statistical analysis of task-based fMRI data and resting-state fMRI data were performed using Statistical Parametric Mapping (SPM12, <http://www.fil.ion.ucl.ac.uk/spm>) implemented in MATLAB (Matlab 7.6, Mathworks, Inc., Concord, MA, USA). fMRI data were preprocessed as follows: 1) head-motion correction, 2) slice-timing correction, 3) coregistration of EPI and T1 images, 4) spatial normalization to the Montreal Neurological Institute 152-brain

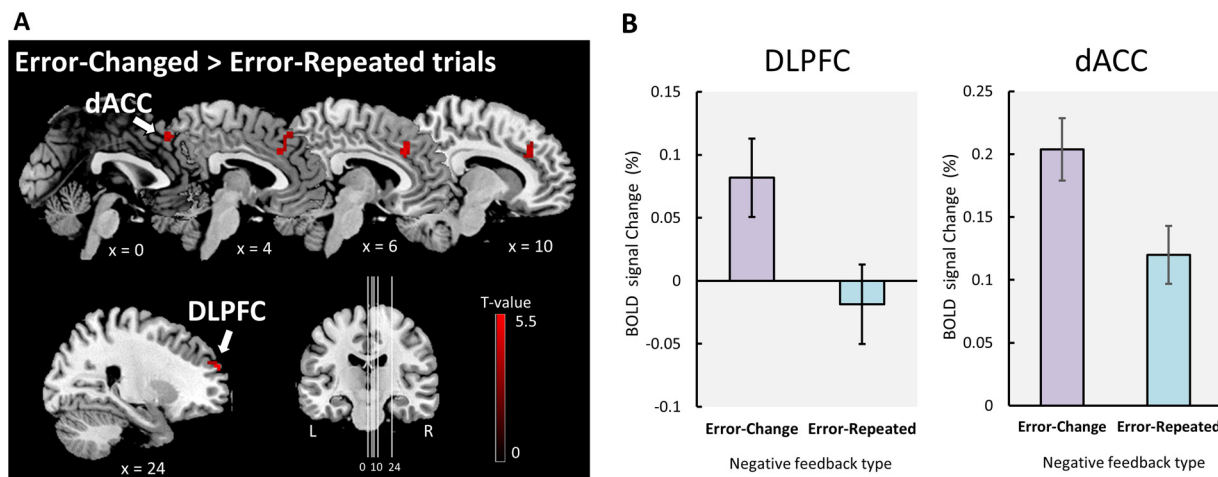


Fig. 2. Task-related fMRI result. (A) Brain regions of error-related activity, differentiating repeated from corrected errors during feedback processing (Error-Changed > Error-Repeated trials). (B) Average BOLD signal changes in the right DLPFC (left) and right dACC (right) in response to 'Error-Changed' and 'Error-Repeated' trials, respectively.

template using T1-image unified segmentation, with a resampling voxel size of $3 \times 3 \times 3 \text{ mm}^3$, 5) spatial smoothing with 6-mm full-width half-maximum.

Negative feedback events were sorted post-hoc into two types; Error-Change and Error-Repeated. Error-Change refers to a negative feedback event of trial n , which was followed by a selection of an alternative response at trial $n + 1$ (for the same letter), while Error-Repeated refers to a negative feedback event of trial n , which was followed by repetition of the same error response at trial $n + 1$. In addition, although it is not the focus of current study, all positive feedback events were modeled into two types: Correct-Repeated (positive feedback event followed by a selection of the same response) and Correct-Changed (positive feedback followed by choice of a different response). The last (fourth) run was excluded from further imaging analysis, because no information on the following response choice was available for half of the feedback events where a letter was presented for the last time (8th repetition), resulting in a total of 144 trials for further analysis. For task-related fMRI analysis, the average number of Error-Changed trials was $59.12 (\pm 9.53)$, and that of Error-Repeated was $18.96 (\pm 6.23)$. Note that both for imaging and behavioral analyses, all negative feedbacks were collapsed, regardless of the size of monetary loss. No significant difference associated with the amount of monetary loss was found either for the correct response rate ($p = 0.92$) or the error adjustment rate ($p = 0.84$). No brain region showed a variation in activation for different size of monetary penalty, even with a lenient threshold (height threshold $p < 0.005$).

In the first-level individual analyses, preprocessed fMRI data were analyzed with a rapid event-related fMRI design, where the four different feedback events (Error-Repeated, Error-Changed, Correct-Repeated, and Correct-Changed) were modeled as regressors. In the general linear model analysis, each regressor was modeled as a stick function (duration = 0 s) convolved with the canonical hemodynamic response function. The six head-motion parameters (three translations and three rotations) derived from realignments were entered as covariates of no interest to remove the effects of head motion. A temporal high-pass filtering with a cut-off frequency $1/128 \text{ Hz}$ was applied to remove low frequency drift, and serial correlations were corrected using a first-order autoregressive model [AR (1)]. The presentation of each learning stimulus, time of response choice, and inter-trial interval, were left un-modeled, serving as implicit baselines. For each participant, only the contrast images for Error-Changed and Error-Repeated events were subjected to a second-level group analysis.

In a second-level random-effect group analysis, a paired t -test was performed between the resultant contrast image of Error-Changed and Error-Repeated in order to identify the brain regions related to

successful error adjustment. We applied a cluster-level, family-wise error (FWE)-corrected p -value of 0.05 for correcting multiple comparisons. First, statistical parametric maps were primarily thresholded at a voxel-level p -value of 0.001. Then a cluster-extent threshold of 297 mm^3 ($k \geq 11$, voxel size = $3 \times 3 \times 3 \text{ mm}$) was applied, which was estimated from 5,000-iteration Monte Carlo simulations implemented in Matlab [29,30]. Brain regions that were considered significant were defined as regions of interest (ROI), and then used for the seed-based analysis in the resting-state fMRI analysis. For illustration purposes, we extracted the percent signal changes of ROI for two negative feedback trial types using the Marsbar toolbox (v0.44, <http://marsbar.sourceforge.net>). The resulting statistical map was superimposed on the MNI template provided by MRICroN software (<http://www.nitrc.org/projects/mricron>). Significant clusters were labeled in accordance with the SPM Anatomy toolbox v2.1 [31].

2.6. Resting-state functional connectivity analysis

2.6.1. Post-hoc definition of ROIs used as seed regions

We examined the resting-state FC associated with two seed regions derived from a task-based fMRI analysis that compared Error-Corrected and Error-Repeated trials. The right DLPFC (BA 46, MNI $x, y, z = 24, 59, 25$, $T = 5.54$, $k = 18$) and right dACC (BA 32, MNI $x, y, z = 6, 29, 34$, $T = 4.97$, $k = 42$) were identified for Error-Changed > Error-Repeated contrast (Fig. 2A).

2.6.2. Preprocessing for resting-state fMRI

Preprocessing for resting-state fMRI was the same as for the task-based fMRI analysis procedure, using statistical parametric mapping (SPM12, <http://www.fil.ion.ucl.ac.uk/spm>). Additional procedures for resting-state fMRI data were performed using the Data Processing Assistant for Resting-State fMRI (DPARSF; V2.3) [32], via the following steps: removal of linear trends; regressing out nuisance covariates (the white matter signal, the cerebrospinal fluid signal, the global signals, and six head-motion parameters); and band-pass temporal filtering ($0.01 - 0.1 \text{ Hz}$).

2.6.3. Resting-state FC-behavioral correlations

For acquiring resting-state FC maps of each ROI, such as the right DLPFC and dACC, we averaged the time-course of all voxels for the seed regions defined by task-based fMRI. For the first-level individual analysis, whole brain correlation maps were generated by calculating the correlation coefficients between the time-course of each voxel across the whole brain and the averaged time-course of the ROIs, respectively, obtaining resting-state FC correlation (r) maps. A Fisher's z -

Table 1

Brain regions showing difference between Error-Changed and Error-Repeated trials.

Brain regions	R/L/M	BA	Cluster size	Peak MNI coordinates			T value
				x	y	z	
Error-Changed > Error-Repeated trials							
DLPFC	R	46	18	24	59	25	5.54
dACC	R	32	42	6	29	34	4.97
dmPFC	M	8		0	35	46	3.87
Error-Changed < Error-Repeated trials							
n.s.							

Cluster-wise FWE corrected $p < 0.05$, Abbreviations: BA, Brodmann's area; MNI, Montreal Neurological Institute; the MNI coordinates and t value for the local maxima of the centers of the clusters; DLPFC, dorsolateral prefrontal cortex; dACC, dorsal anterior cingulate cortex; dmPFC, dorsomedial prefrontal cortex; n.s., non-significant. Italics used to emphasize that dmPFC was part of the cluster of the dACC.

transformation was used to normalize the individual correlation maps to z-maps. For the group level analysis, resting-state FC-behavior analyses were carried out to identify brain regions for which the intrinsic FC of the right DLPFC and dACC at rest predicted individual behavioral adjustment performance. A whole-brain regression analysis with the behavioral adjustment ratio as covariates in the right DLPFC and dACC z-maps was performed (Table 2 and Table S1). The resulting maps were determined by a voxel-level height threshold with $p < 0.001$, with an extent threshold of 297 mm^3 ($k \geq 11$, voxel size = 3 mm^3). For both task-based fMRI and resting-state correlation analysis, we also report the brain regions that survived a more conservative multiple correction threshold, voxel-wise FWE correction of $p < 0.05$, in Table 1 and 2.

3. Results

3.1. Behavioral results

Performance of stimulus–response associations significantly improved across the four runs, $F_{(3, 75)} = 144.901$, $p < 0.0001$. The mean CRs was 31.31% ($SD = 6.10$) for the first run, 47.23% ($SD = 9.00$) for the second run, 58.96% ($SD = 12.16$) for the third run, and 70.90% ($SD = 13.59$) for the last run.

The average of the error adjustment rate across all participants was 75.79% ($SD = 6.15$), ranging from 60.00% to 89.09%, indicating that there was relatively high individual variability. There was, however, no significant run effect on the error adjustment rate, $F_{(1, 25)} = 1.47$, $p = 0.23$, indicating constancy of error adjustment rate across runs. The mean response times for Error-Changed trials ($M = 1199.32 \text{ ms}$, $SD = 127.22$) did not differ from those for Error-Repeated trials ($M = 1212.63 \text{ ms}$, $SD = 148.84$), $t(25) = -0.69$, $p = 0.50$. No difference was found between the length of the delay period between two consecutive learning stimuli [$t(25) = -0.401$, $p = 0.692$; for error-

changed trials, $M = 251.64 \text{ s}$, $SD = 7.07$; for error-repeated trials, $M = 253.20 \text{ s}$, $SD = 14.60$], indicating that delay length did not affect the success or failure of subsequent behavioral adjustment of error response. For positive feedback, 80.98% ($SD = 9.8$) of the rewarded trials were followed by repetition of the correct response in the subsequent trial, indicating stable learning performance.

3.2. fMRI comparison of Error-Changed and Error-Repeated trials

The paired *t*-test analysis revealed a significant difference between Error-Changed trials and Error-Repeated trials in the right DLPFC and right dACC. For those brain regions, greater activations were observed when subsequent adaptive behavioral alterations occurred relative to when the error was repeated (Error-Changed > Error-Repeated trials; Fig. 2B). In particular, the results for the dACC were consistent with those of a previous study [32], showing that the error-related dACC response was related to behavioral adjustment. The magnitude of the BOLD percent signal change for Error-Changed trials was not correlated with individual differences in error adjustment rates in either the right DLPFC ($r[24] = -0.15$, $p = 0.48$) or the right dACC ($r[24] = 0.04$, $p = 0.83$). Significant positive correlations between the right DLPFC and right dACC activities were found for Error-Changed trials, $r(24) = .46$, $p = 0.016$, not for Error-Repeated trial, $r(24) = .01$, $p = 0.95$.

3.3. Correlation between resting-state FC and behavior

In a whole-brain regression analysis of the DLPFC, significant negative correlations with individual differences in error adjustment were found in the right paracentral lobule and left inferior temporal region extending to the hippocampus (Table 2, Fig. 3A). Specifically, individuals with better error performance showed a strong negative correlation between the DLPFC and paracentral lobule, and between the DLPFC and the inferior temporal region.

Also, the strength of FC between the dACC and amygdala was negatively correlated with the error adjustment ratio (Table 2, Fig. 3B). Individuals with a higher positive FC between the dACC and the right amygdala showed lower adjustment rates for error, whereas those with negative FC between the dACC and the amygdala showed higher adjustment performance.

4. Discussion

Although the dACC has been considered a critical region in error processing, it has not been clear to what extent the resting-state FC of this brain region affects individual differences in error-feedback processing efficiency. In the current study, we examined error-adjustment related brain regions for which resting-state FC was correlated with the ability to perform error processing. We found that the right dACC and right DLPFC were associated with successful error and feedback

Table 2

Functional connectivity predicted by error adjustment rate.

Seed Region	Correlation	Regions	L/R/M	BA	Cluster size	Peak MNI coordinate			T value
						x	y	z	
Right DLPFC	negative	paracentral lobule	R	4	71	9	-25	79	8.13*
		inferior temporal gyrus							
Right dACC	positive	hippocampus		20	32	-42	-19	-35	6.86*
		n.s.							
Right dACC	negative	amygdala	R	34	15	21	-8	17	4.25
		n.s.							

Cluster-wise FWE corrected $p < 0.05$; * refers to voxel-wise FWE-corrected $p < 0.05$. Abbreviations: BA, Brodmann's area; MNI, Montreal Neurological Institute; the MNI coordinates and t value for the local maxima of the centers of the clusters; DLPFC, dorsolateral prefrontal cortex; dACC, dorsal anterior cingulate cortex; n.s., non-significant. Italics used for hippocampal data to emphasize that hippocampus was part of the cluster of the inferior temporal gyrus.

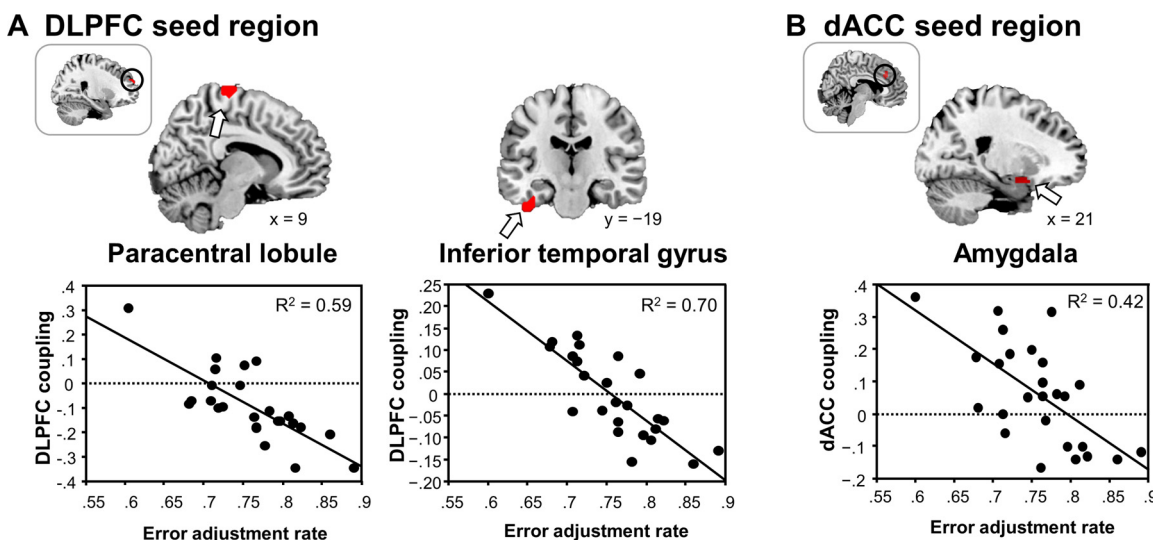


Fig. 3. Brain regions showing strength of resting-state functional connectivity (FC) as functions of an error-adjustment rate. (A) Functional connectivity between the DLPFC and paracentral lobule (left), and between the DLPFC and an area consisting of inferior temporal and adjacent hippocampal regions (right) were negatively correlated with the error adjustment rate. (B) The strength of dACC – amygdala connectivity was negatively correlated with error adjustments.

processing. Moreover, better error adjustment performance was associated with a stronger negative correlation between the DLPFC seed and the paracentral gyrus, between the DLPFC seed and the hippocampus, and between the right dACC seed and the amygdala.

In the feedback-based learning task, individual variability ranged from 60.00% to 89.09% in terms of error adjustment efficiency in the normal young adult participants. Individual ability was constant during the learning task, with no improvement in the error adjustment ratio, while CRs rates increased as learning occurred across runs. Assuming these properties to be continuous and constant, rather than dichotomous, the approach that we applied in resting-state FC-behavior correlation analysis is appropriate for investigations of intrinsic resting-state FC related to adjustment ability. In addition, it should be noted that some participants had a ratio of Error-Changed trials of less than 75%. Although, given four response options, the chance level was 75% for Error-Changed, some participants had a ratio below 75%, indicating that these participants tended to select the previously punished button. This suggests that a strong stimulus-response association was formed, even though it was for the wrong pairs. Although the average error adjustment rate across all participants was 75.79%, the error adjustment rates of each individual participant were distributed across a wide range, including those in the upper tail of the distribution who adjusted their errors appropriately with information obtained by negative feedback, as well as those in the lower tail who repeatedly produced the same erroneous response.

The increased dACC activation in Error-Changed trials, as compared to Error-Repeated trials, was consistent with previous studies that revealed that the magnitude of error-related pMFC activity is related to adaptive post-error behavior [33,34]. Higher dACC activation in response to negative feedback relative to positive feedback has also been reported [13,35]. Our results confirm that the dACC is involved in successful error processing, and may inhibit a punished erroneous response and promote exploration of alternative subsequent responses [36]. Our findings also support a role for the dACC in reinforcement learning [37], suggesting that a negative reinforcement signal, conveyed to the dACC from the mesencephalic dopamine system, is used to correct and modify performance [38].

During Error-Changed trials, increased dACC activity was accompanied by a similar effect in another region, the DLPFC. Previous studies of feedback processing have also reported increased activity in the DLPFC in response to negative feedback, relative to the response to positive feedback [13,39]. For example, Zanolie, Van Leijenhorst,

Rombouts and Crone [13] showed that the DLPFC is sensitive to feedback information provided for future actions, suggesting that the DLPFC plays a role in goal-directed behavior. Patients with lateral PFC lesions are often described as being perseverative, showing impaired inhibition of incorrect behavior, which might reflect an impairment in behavior adjustment [40]. Given that negative feedback indicated to participants that the current association between the alphabet stimulus and their response was incorrect, one strategy for successful error adjustment could be to maintain the relevant information, such as their response and the associated outcomes, and to update or inhibit irrelevant information based on the feedback. The DLPFC has been consistently implicated as subservient to cognitive control, such as manipulation of working memory [41]. Studies linking DLPFC activity to working memory are relevant in this respect, given that working memory demands increase after negative feedback [42].

Considering previous findings, our results not only indicate a consistent role of the DLPFC in working memory during feedback-based learning [42], but also suggest that error-related DLPFC activity is important for subsequent behavioral adjustments. However, inter-individual variability in error adjustment ability was not correlated with the degree of dACC and DLPFC activation itself. Instead, the FC analysis using a dACC seed region showed that increased anticorrelated FC between the dACC and amygdala is related to better error adjustment ability. It is well established that the amygdala plays a central role in detecting and encoding emotional information, and provides contextual information to cortical regions for adjusting motivational levels [43]. For example, previous studies have identified amygdala activity in response to negative events, such as monetary loss during aversive learning [44], with the level of activity linked to avoiding negative outcomes [45]. These findings suggest that the amygdala plays a key role in generating loss aversion by inhibiting actions that have potentially deleterious outcomes [46]. In particular, the connectivity of the amygdala and frontal cortex regions, such as the dACC, is known to play an important role in adjusting negative emotion with reciprocal anatomical connections [47,48]. Anticorrelated FC between the medial prefrontal cortex encompassing the dACC and amygdala is one of the features observed during development [49]. Reduced negative connectivity between these frontal regions and the amygdala has been found in disorders that involve emotional processing and emotional regulation deficits, including major depression [50]. Dysregulated interaction between the dACC and amygdala may be related to a negative processing bias, and this will manifest as a defective disengagement

from enhanced attentional capture and negative events.

The paracentral lobule is one of the brain regions in the default mode network, which is thought to support a general pattern of task-independent cognitive resources during rest [51]. Given that the DLPFC is considered the task-positive network, our results indicate a strong anti-correlation between a task-positive network and a task-negative network related to improved performance in error correction. As greater anticorrelation between the medial prefrontal cortex and DLPFC is known to be related to better working memory capacity [52], it appears that variability of error adjustment depends on utility of working memory.

In addition to the paracentral lobule regions, the strength of FC between the DLPFC and the inferior temporal region extending to the hippocampus was also related to individual variability in error adjustment performance. Many studies have reported hippocampal deactivation in instrumental learning [53,54]. For instance, hippocampal deactivation is related to learning success, and those activations are negatively correlated with striatal activation during learning from feedback [55]. The relationship between the hippocampus and striatum is known to be antagonistic [56], especially in striatum-dependent learning, that is, in feedback-driven learning, which is similar to our paradigm. Although recent studies have reported a role of the hippocampus in feedback-driven learning [57], the hippocampus may play a critical role only when feedback is received after a long delay (i.e., 7 s), rather than immediately, as in our study. Using the FC approach, Poldrack and Rodriguez [58] showed that the prefrontal cortex plays supervisory roles by mediating the interaction between two brain systems, particularly with the negative path from the DLPFC to the medial temporal lobe. Consistent with their results, the strong negative intrinsic FC between the DLPFC and hippocampus in participants with better error adjustments observed in the present study may reflect a strong regulatory role of the DLPFC over the hippocampus.

The use of task-based fMRI to identify brain regions involved in successful and unsuccessful processing, and the application of resting-state FC using such functionally well-defined regions as seed regions, are strengths of the current study. However, the literature on potential limitations of seed-based FC identifies analytical pitfalls that must be considered (e.g., seed selection) [59]. Because seed-based analysis is a hypothesis-driven method based on an *a priori* decision, the results could be suspect, depending on the specific seed regions. Unlike many seed-based approaches that are guided by a priori hypothesis, we selected representative seeds that were extracted from task-based fMRI data during learning. By using a combination of these two approaches, we were able to address the limitation of seed-based FC analysis.

Finally, a number of studies provide evidence of developmental differences in learning from error [60–61]. The participants of the present study were all young adults, so one should be cautious in generalizing our results to other age groups.

5. Conclusions

Our results suggest that individual variability in learning from error depends on intrinsic connectivity between brain regions that have been implicated in error processing, emotional processing, and motor processing. Specifically, a strong negative relationship of the dACC-related network with the emotion-related network (i.e., amygdala) in individuals with higher error adjustment rates suggests that controlling the effect of emotion on error processing is an important factor for better performance in negative feedback learning. More broadly, our results provide evidence that FC variability may be an important factor underlying individual differences in error adjustment during feedback-based learning.

Acknowledgements

This work was supported by the Brain Research Program of the

National Research Foundation of Korea, Ministry of Science and ICT (NRF-2006-2005112) to E.K.

Appendix A. Supplementary data

Supplementary data associated with this article can be found, in the online version, at <https://doi.org/10.1016/j.bbr.2018.02.024>.

References

- [1] M. Ullsperger, D.Y. von Cramon, Error monitoring using external feedback: specific roles of the habenular complex, the reward system, and the cingulate motor area revealed by functional magnetic resonance imaging, *J. Neurosci.* 23 (10) (2003) 4308–4314.
- [2] C.S. Carter, T.S. Braver, D.M. Barch, M.M. Botvinick, D. Noll, J.D. Cohen, Anterior cingulate cortex, error detection, and the online monitoring of performance, *Science* 280 (5364) (1998) 747–749.
- [3] M. Han, L. Shi, S. Jia, Attentional resources modulate error processing-related brain electrical activity evidence from a dual-task design, *Brain Res.* (2017).
- [4] D.G. Ghahremani, J. Monterosso, J.D. Jentsch, R.M. Bildner, R.A. Poldrack, Neural components underlying behavioral flexibility in human reversal learning, *Cereb. Cortex* 20 (8) (2009) 1843–1852.
- [5] K. Jimura, S. Konishi, T. Asari, Y. Miyashita, Involvement of medial prefrontal cortex in emotion during feedback presentation, *Neuroreport* 20 (9) (2009) 886–890.
- [6] M.J. Frank, L.C. Seeberger, R.C. O'Reilly, By carrot or by stick: cognitive reinforcement learning in parkinsonism, *Science* 306 (5703) (2004) 1940–1943.
- [7] M.F. Rushworth, M.J. Buckley, T.E. Behrens, M.E. Walton, D.M. Bannerman, Functional organization of the medial frontal cortex, *Curr. Opin. Neurobiol.* 17 (2) (2007) 220–227.
- [8] S.F. Taylor, E.R. Stern, W.J. Gehring, Neural systems for error monitoring: recent findings and theoretical perspectives, *Neuroscientist* 13 (2) (2007) 160–172.
- [9] S. de Wit, P. Watson, H.A. Harsay, M.X. Cohen, I. van de Vijver, K.R. Ridderinkhof, Corticostriatal connectivity underlies individual differences in the balance between habitual and goal-directed action control, *J. Neurosci.* 32 (35) (2012) 12066–12075.
- [10] S. Nieuwenhuis, C.B. Holroyd, N. Mol, M.G. Coles, Reinforcement-related brain potentials from medial frontal cortex: origins and functional significance, *Neurosci. Biobehav. Rev.* 28 (4) (2004) 441–448.
- [11] C.B. Holroyd, S. Nieuwenhuis, N. Yeung, L. Nystrom, R.B. Mars, M.G. Coles, J.D. Cohen, Dorsal anterior cingulate cortex shows fMRI response to internal and external error signals, *Nat. Neurosci.* 7 (5) (2004) 497–498.
- [12] R.B. Mars, M.G.H. Coles, M.J. Grol, C.B. Holroyd, S. Nieuwenhuis, W. Hulstijn, I. Toni, Neural dynamics of error processing in medial frontal cortex, *Neuroimage* 28 (4) (2005) 1007–1013.
- [13] K. Zanolie, L. Van Leijenhorst, S.A. Rombouts, E.A. Crone, Separable neural mechanisms contribute to feedback processing in a rule-learning task, *Neuropsychologia* 46 (1) (2008) 117–126.
- [14] K.C. Bickart, B.C. Dickerson, L. Feldman Barrett, The amygdala as a hub in brain networks that support social life, *Neuropsychologia* 63 (2014) 235–248.
- [15] T.A. Klein, J. Neumann, M. Reuter, J. Hennig, D.Y. von Cramon, M. Ullsperger, Genetically determined differences in learning from errors, *Science* 318 (5856) (2007) 1642–1645.
- [16] M.J. Frank, B.S. Woroch, T. Curran, Error-related negativity predicts reinforcement learning and conflict biases, *Neuron* 47 (4) (2005) 495–501.
- [17] D.L. Santesso, D.G. Dillon, J.L. Birk, A.J. Holmes, E. Goetz, R. Bogdan, D.A. Pizzagalli, Individual differences in reinforcement learning: behavioral, electrophysiological, and neuroimaging correlates, *NeuroImage : Clin.* 42 (2) (2008) 807–816.
- [18] R.L. Buckner, F.M. Krienen, B.T. Yeo, Opportunities and limitations of intrinsic functional connectivity MRI, *Nat. Neurosci.* 16 (7) (2013) 832–837.
- [19] W.W. Seeley, V. Menon, A.F. Schatzberg, J. Keller, G.H. Glover, H. Kenna, A.L. Reiss, M.D. Greicius, Dissociable intrinsic connectivity networks for salience processing and executive control, *J. Neurosci.* 27 (9) (2007) 2349–2356.
- [20] B. Biswal, F. Zerrin Yetkin, V.M. Haughton, J.S. Hyde, Functional connectivity in the motor cortex of resting human brain using echo-planar MRI, *Magn. Reson. Med.* 34 (4) (1995) 537–541.
- [21] D. Cordes, V.M. Haughton, K. Arfanakis, G.J. Wendt, P.A. Turski, C.H. Moritz, M.A. Quigley, M.E. Meyerand, Mapping functionally related regions of brain with functional connectivity MR imaging, *Am. J. Neuroradiol.* 21 (9) (2000) 1636–1644.
- [22] A. Baldassarre, C.M. Lewis, G. Committeri, A.Z. Snyder, G.L. Romani, M. Corbetta, Individual variability in functional connectivity predicts performance of a perceptual task, *Proc. Natl. Acad. Sci. U. S. A.* 109 (9) (2012) 3516–3521.
- [23] M. Hampson, N.R. Driesen, P. Skudlarski, J.C. Gore, R.T. Constable, Brain connectivity related to working memory performance, *J. Neurosci.* 26 (51) (2006) 13338–13343.
- [24] X. Wang, Z. Han, Y. He, L. Liu, Y. Bi, Resting-state functional connectivity patterns predict Chinese word reading competency, *PLoS One* 7 (9) (2012) e44848.
- [25] M. Hampson, N. Driesen, J.K. Roth, J.C. Gore, R.T. Constable, Functional connectivity between task-positive and task-negative brain areas and its relation to working memory performance, *Magn. Reson. Imaging* 28 (8) (2010) 1051–1057.
- [26] A. Kelly, L.Q. Uddin, B.B. Biswal, F.X. Castellanos, M.P. Milham, Competition between functional brain networks mediates behavioral variability, *Neuroimage* 39

(1) (2008) 527–537.

[27] L.Q. Uddin, A. Clare Kelly, B.B. Biswal, F. Xavier Castellanos, M.P. Milham, Functional connectivity of default mode network components: correlation, anticorrelation, and causality, *Hum. Brain Mapp.* 30 (2) (2009) 625–637.

[28] A.M. Dale, Optimal experimental design for event-related fMRI, *Hum. Brain Mapp.* 8 (2–3) (1999) 109–114.

[29] S.D. Slotnick, Cluster success: fMRI inferences for spatial extent have acceptable false-positive rates, *Cogn. Neurosci.* 8 (3) (2017) 150–155.

[30] S.D. Slotnick, L.R. Moo, J.B. Segal, J. Hart, Distinct prefrontal cortex activity associated with item memory and source memory for visual shapes, *Cognit. Brain Res.* 17 (1) (2003) 75–82.

[31] S.B. Eickhoff, K.E. Stephan, H. Mohlberg, C. Grefkes, G.R. Fink, K. Amunts, K. Zilles, A new SPM toolbox for combining probabilistic cytoarchitectonic maps and functional imaging data, *Neuroimage* 25 (4) (2005) 1325–1335.

[32] Y. Chao-Gan, Z. Yu-Feng, DPARSF: A MATLAB toolbox for “Pipeline” data analysis of resting-state fMRI, *Front. Syst. Neurosci.* 4 (2010) 13.

[33] R. Hester, N. Barre, K. Murphy, T.J. Silk, J.B. Mattingley, Human medial frontal cortex activity predicts learning from errors, *Cereb. Cortex* 18 (8) (2008) 1933–1940.

[34] R. Hester, K. Murphy, F.L. Brown, A.J. Skilleter, Punishing an error improves learning: the influence of punishment magnitude on error-related neural activity and subsequent learning, *J. Neurosci.* 30 (46) (2010) 15600–15607.

[35] J. Wang, B. Cao, X. Cai, H. Gao, F. Li, Brain activation of negative feedback in rule acquisition revealed in a segmented wisconsin card sorting test, *PLoS One* 10 (10) (2015) e0140731.

[36] R. Quilodran, M. Rothe, E. Procyk, Behavioral shifts and action valuation in the anterior cingulate cortex, *Neuron* 57 (2) (2008) 314–325.

[37] C.B. Holroyd, M.G. Coles, The neural basis of human error processing: reinforcement learning, dopamine, and the error-related negativity, *Psychol. Rev.* 109 (4) (2002) 679–709.

[38] M. Matsumoto, K. Matsumoto, H. Abe, K. Tanaka, Medial prefrontal cell activity signaling prediction errors of action values, *Nat. Neurosci.* 10 (5) (2007) 647–656.

[39] A.C. van Duijvenvoorde, K. Zanolie, S.A. Rombouts, M.E. Rajmakers, E.A. Crone, Evaluating the negative or valuing the positive? neural mechanisms supporting feedback-based learning across development, *J. Neurosci.* 28 (38) (2008) 9495–9503.

[40] F. Barcelo, R.T. Knight, Both random and perseverative errors underlie WCST deficits in prefrontal patients, *Neuropsychologia* 40 (3) (2002) 349–356.

[41] A. Bari, T.W. Robbins, Inhibition and impulsivity: behavioral and neural basis of response control, *Prog. Neurobiol.* 108 (2013) 44–79.

[42] A.G. Collins, M.J. Frank, How much of reinforcement learning is working memory, not reinforcement learning? A behavioral, computational, and neurogenetic analysis, *Eur. J. Neurosci.* 35 (7) (2012) 1024–1035.

[43] J.J. Paton, M.A. Belova, S.E. Morrison, C.D. Salzman, The primate amygdala represents the positive and negative value of visual stimuli during learning, *Nature* 439 (7078) (2006) 865–870.

[44] M.R. Delgado, C.D. Labouliere, E.A. Phelps, Fear of losing money? Aversive conditioning with secondary reinforcers, *Soc. Cogn. Affect. Neurosci.* 1 (3) (2006) 250–259.

[45] M. Delgado, R. Jou, J. LeDoux, L. Phelps, Avoiding negative outcomes: tracking the mechanisms of avoidance learning in humans during fear conditioning, *Front. Behav. Neurosci.* 3 (33) (2009).

[46] B. De Martino, C.F. Camerer, R. Adolphs, Amygdala damage eliminates monetary loss aversion, *Proc. Natl. Acad. Sci. U. S. A.* 107 (8) (2010) 3788–3792.

[47] H.T. Ghashghaei, C.C. Hilgetag, H. Barbas, Sequence of information processing for emotions based on the anatomic dialogue between prefrontal cortex and amygdala, *Neuroimage* 34 (3) (2007) 905–923.

[48] B.A. Vogt, D.N. Pandya, Cingulate cortex of the rhesus monkey: II. Cortical afferents, *J. Comp. Neurol.* 262 (2) (1987) 271–289.

[49] D.G. Gee, K.L. Humphreys, J. Flannery, B. Goff, E.H. Telzer, M. Shapiro, T.A. Hare, S.Y. Bookheimer, N. Tottenham, A developmental shift from positive to negative connectivity in human amygdala–prefrontal circuitry, *J. Neurosci.* 33 (10) (2013) 4584–4593.

[50] H.S. Mayberg, M. Liotti, S.K. Brannan, S. McGinnis, R.K. Mahurin, P.A. Jerabek, J.A. Silva, J.L. Tekell, C.C. Martin, J.L. Lancaster, P.T. Fox, Reciprocal limbic–cortical function and negative mood: converging PET findings in depression and normal sadness, *Am. J. Psychiatry* 156 (5) (1999) 675–682.

[51] M.D. Greicius, B. Krasnow, A.L. Reiss, V. Menon, Functional connectivity in the resting brain: a network analysis of the default mode hypothesis, *Proc. Natl. Acad. Sci. U. S. A.* 100 (1) (2003) 253–258.

[52] J.B. Keller, T. Heden, T.W. Thompson, S.A. Anteraper, J.D.E. Gabrieli, S. Whitfield-Gabrieli, Resting-state anticorrelations between medial and lateral prefrontal cortex: association with working memory, aging, and individual differences, *Cortex; J. Devoted Study Nerv. Syst. Behav.* 64 (2015) 271–280.

[53] K.R. Luking, D.M. Barch, Candy and the brain: neural response to candy gains and losses, *Cogn. Affect. Behav. Neurosci.* 13 (3) (2013) 437–451.

[54] C.A. Seger, C.M. Cincotta, Dynamics of frontal, striatal, and hippocampal systems during rule learning, *Cereb. Cortex* 16 (11) (2006) 1546–1555.

[55] R.A. Poldrack, J. Clark, E.J. Pare-Blagoev, D. Shohamy, J. Crespo Moyano, C. Myers, M.A. Gluck, Interactive memory systems in the human brain, *Nature* 414 (6863) (2001) 546–550.

[56] K. Foerde, E. Race, M. Verfaellie, D. Shohamy, A role for the medial temporal lobe in feedback-driven learning: evidence from amnesia, *J. Neurosci.* 33 (13) (2013) 5698–5704.

[57] R.A. Poldrack, P. Rodriguez, How do memory systems interact? evidence from human classification learning, *Neurobiol. Learn. Mem.* 82 (3) (2004) 324–332.

[58] D.M. Cole, S.M. Smith, C.F. Beckmann, Advances and pitfalls in the analysis and interpretation of resting-state fMRI data, *Front. Syst. Neurosci.* 4 (2010).

[59] N.A. Dennis, R. Cabeza, Age-related dedifferentiation of learning systems: an fMRI study of implicit and explicit learning, *Neurobiol. Aging* 32 (12) (2011) 2318 e17–30.

[60] M.J. Frank, L. Kong, Learning to avoid in older age, *Psychol. Aging* 23 (2) (2008) 392.

[61] I. van de Vijver, K.R. Ridderinkhof, S. de Wit, Age-related changes in deterministic learning from positive versus negative performance feedback, *Neuropsychol. Dev. Cognition Sect. B Aging Neuropsychol. Cognition* 22 (5) (2015) 595–619.